

## Microwave Absorbing Properties of Polyaniline-NiFe<sub>2</sub>O<sub>4</sub>: V composites

<sup>1</sup>Ethem Ilhan SAHIN and <sup>2</sup>Selcuk PAKER <sup>3</sup>Mesut KARTAL\*

<sup>1</sup>Satellite Communications and Remote Sensing, Istanbul Technical University, Maslak, Istanbul, Turkey.

<sup>2,3</sup>Electronics and Communication Engineering Department (“Department of Electronics and Communication Engineering”), Istanbul Technical University, Maslak, Istanbul, Turkey.

kartalme@itu.edu.tr\*

(Received on 27<sup>th</sup> April 2018, accepted in revised form 3<sup>rd</sup> September 2018)

**Summary:** In this study, vanadium doped NiFe<sub>2</sub>O<sub>4</sub> was produced by using mixed oxide technique. The NiFe<sub>2-x</sub>V<sub>x</sub>O<sub>4</sub> composition was synthesized and x was selected as 0.1, 0.2 and 0.3, respectively. The single-phase Ni ferrite was produced after sintering at 1100°C for 4h. X-Ray diffraction (XRD), scanning electron microscopy (SEM) and energy-dispersive X-ray spectroscopy (EDS) were performed for structural analysis. The results of the structural analysis indicated that the second phase did not form in NiFe<sub>2-x</sub>V<sub>x</sub>O<sub>4</sub>. Additionally, the polyaniline-vanadium doped NiFe<sub>2</sub>O<sub>4</sub> composites were produced by hot pressing using the compositions of NiFe<sub>1.9</sub>V<sub>0.1</sub>O<sub>4.1</sub>, NiFe<sub>1.8</sub>V<sub>0.2</sub>O<sub>4.2</sub>, NiFe<sub>1.7</sub>V<sub>0.3</sub>O<sub>4.3</sub>, and aniline. The weight ratios of vanadium-doped nickel ferrite and aniline were 1:1 and 1:3, respectively. Epoxy resin was used to produce microwave-absorbing composites. The fabricated composites were characterized by using Fourier transform infrared spectroscopy (FTIR). Furthermore, the magnetic properties of the fabricated composites were investigated by using a vibrating sample magnetometer (VSM). The microwave absorbing performances of the polyaniline-NiFe<sub>2</sub>O<sub>4</sub>: V composites were investigated by reflectivity in 0–8 GHz, using a two-port vector network analyzer. A minimum of -42.17 dB reflection performance was obtained in 7.02 GHz at the thickness of 2.0 mm. This reflection performance can be modulated simply by controlling the content of polyaniline in the samples for the required frequency bands.

**Keywords:** Microwave absorber, NiFe<sub>2</sub>O<sub>4</sub>, Polyaniline, Polymer-matrix composites, Reflectivity.

### Introduction

The extraordinary growth in the communications industry has led to an increased interest in microwave absorbing materials. With modern communication systems recently diving into high frequency, the interest and need for absorbing materials suitable for using in high frequency has naturally increased [1]. The interest in microwave absorbing materials because of the rapid progress of wireless communication has also become more notable in applications outside of various specific areas such as radar systems and military applications [2]. It is also known today that the electromagnetic pollution for this reason caused by the signals spreading from electronic devices, which are becoming increasingly widespread for their usage, has many negative consequences on human health and the environment [3]. Studies on absorbing materials are continuously carried out in order to overcome these problems, minimize the electromagnetic effects, and provide safety in the areas of radar, space technology, telecommunication, local area networks, military and communication technologies [4, 5].

The decline in electromagnetic energy by using the microwave theory can be attributed to the large number of internal reflections caused by the material itself [6], it is necessary that the incoming

signal to absorbing material should not reflect to the incoming direction and should not provide transmission at the same time. Thus, the signal has to provide absorption in or on the material.

Nano spinel ferrites [7] generally described by the formula AFe<sub>2</sub>O<sub>4</sub> (A= divalent metal ion, Mg, Ni, Co, Cu, etc.), have superparamagnetic behavior and, due to their interesting properties, have intensively investigated for magnetic fluids, gas sensor, applications in the magnetic information storage systems, catalysts, magnetic resonance imaging and microwave devices operating in high frequency range [8 and 15].

The spinel ferrites in the NiFe<sub>2</sub>O<sub>4</sub> structure can be used as EM wave absorbers due to their high magnetic losses and resistivity. Although they are also particularly attractive to researchers due to their high magnetocrystalline anisotropy, high saturation magnetization and unique magnetic structure needs to be reworded [16].

NiFe<sub>2</sub>O<sub>4</sub> has an inverse spinel structure showing ferrimagnetism due to the magnetic moment of the anti-parallel spins between the Fe<sup>+3</sup> ions in tetrahedral region and the Ni<sup>+2</sup> ions in the octahedral region [17]. The properties of these spinel ferrites

---

\*To whom all correspondence should be addressed.

vary according to their chemical composition, microstructure, stoichiometry, ion position doped by sintering parameters, and contribution ratio [18]. Additionally, in recent years studies have been conducted on the absorber-based ferromagnetic materials such as Ni/ZnO [19], Co/ZnO [20], Fe/ZnO [21],  $\text{FeNi}_3/(\text{Ni}_{0.5}\text{Zn}_{0.5})\text{Fe}_2\text{O}_4$  [22] and Fe/SiO<sub>2</sub> [23].

As a microwave absorbing material, NiFe<sub>2</sub>O<sub>4</sub> has disadvantages such as small dielectric loss and wide area density, and this limits the potential of NiFe<sub>2</sub>O<sub>4</sub> for using in wideband absorption bandwidth applications [24-25]. Although NiFe<sub>2</sub>O<sub>4</sub> has microwave absorption properties, it is quite heavy, however the ferrite polymer composites obtained by mixing pure ferrite powders with non-magnetic polymers for better absorption properties show better microwave properties depending on low cost, lightness and good design flexibility [26-28]. Magnetic materials and composites containing conductive polymers in order to obtain high efficiency microwave absorbers with strong absorption and wide band spacing, having thin layer and light weight, have attracted a great deal of interest from researchers due to the hybrid nature of each compound [29].

Polyaniline (PANI), whose microwave absorbing properties are associated with its structure, is a promising conductive polymer with excellent chemical and physical properties, low cost, good environmental stability [30]. PANI can be prepared easily by the chemical oxidative polymerization of aniline under controlled conditions and exhibits sufficient stability for practical applications. The chemical method from these methods is more common. The preparation method is oxidative polymerization with ammonium sulfate as an oxidant in general.

The mechanical and other properties of PANI may increase depending on the additives in which a mixture of inorganic nanomaterials and PANI is used. It has been found that the composites have good magnetic, conductivity and microwave absorbing properties in the studies conducted regarding composites containing conductive polymer and magnetic ferrite.

Protective materials with reflection loss using intrinsic conductive polymer (ICP) are very promising. Compared to intrinsic conductive polymers, PANI not only has specified reflective loss, but also has more absorption loss to achieve the electromagnetic shielding. Therefore, it can meet the high absorption and low reflection need [31-32].

In previous studies, the microwave absorbing properties of PANI-MnFe<sub>2</sub>O<sub>4</sub> nanocomposite powders dispersed in acrylic resin with a coating thickness of 1.4 mm were measured using a vector network analyzer at a frequency range of 8-12 GHz, and its minimum reflection loss was measured as -15.3 dB at 10.4 GHz [33]. In addition, the reflection losses of the PANI-C<sub>0.7</sub>Cr<sub>0.1</sub>Zn<sub>0.2</sub>Fe<sub>2</sub>O<sub>4</sub> composites were measured as -13.17 dB and -15.36 dB at 14.1 GHz and 17.9 GHz, respectively [34]. On the other hand, the reflection losses of the prepared PANI-BaFe<sub>12</sub>O<sub>19</sub> composites were measured as -12.5 dB and -11.5 dB at 7.8 GHz and 24.2 GHz, respectively [35]. For example, in another study, ZnO-PANI composite has a width of 3.5 mm sample thickness and a maximum -41 dB reflection loss at 14.1 GHz frequency [36].

A good absorbing material should have broad bandwidth, wide frequency range, strong absorption and should be lightweight and thin as well [37]. Electromagnetic wave can be characterized based on its absorption properties and coefficient of reflection. Dielectric loss, magnetic loss and impedance match factors are considered on the design principle of EM absorbing materials [38].

-10 dB RL (reflection loss) can be compared with 90% microwave absorption. Therefore, the materials with a RL value less than -10 dB are considered to be suitable electromagnetic wave absorbers. [39].

Using polyaniline based V doped NiFe<sub>2</sub>O<sub>4</sub> composite, production of light and thin high performance electromagnetic wave absorption material with wide absorption band and powerful absorption performance is planned. With V doping, reducing sintering temperature and improving the microwave absorption property of NiFe<sub>2</sub>O<sub>4</sub> in polyaniline composite was aimed. Using the simple method of oxide mixing, a new single phase V doped NiFe<sub>2</sub>O<sub>4</sub> was formed, V doping was investigated, by adding special rates of V doping to NiFe<sub>2</sub>O<sub>4</sub>, V doped NiFe<sub>2</sub>O<sub>4</sub> : PANI based composite was formed and its microwave absorption properties was investigated.

The single phase NiFe<sub>2</sub>O<sub>4</sub> ferrites were prepared by means of mixing oxides by adding V as solid solution in different ratios instead of Fe in the NiFe<sub>2</sub>O<sub>4</sub> ferrite composition for the first time in this study. To our knowledge this study is the first to measure the microwave absorber properties of the V-doped Nickel ferrite: PANI composite. The amounts of the initial oxides were calculated based on

stoichiometric composition of  $\text{NiFe}_{2-x}\text{V}_x\text{O}_4$ . The solubility limit, which is defined as the amount that can be doped without disturbing the structure of the main structure ( $\text{NiFe}_2\text{O}_4$ ), was determined using X-ray powder diffractometry. SEM results were investigated, the magnetic hysteresis measurement (VSM) results of the V-doped  $\text{NiFe}_2\text{O}_4$  ferrites and the V-doped  $\text{NiFe}_2\text{O}_4$ : PANI were determined.

When sintered at high temperatures, the structure of  $\text{NiFe}_2\text{O}_4$  is disrupted. The single-phase  $\text{NiFe}_2\text{O}_4$  ferrites were sintered between at  $1200^\circ\text{C}$ - $1300^\circ\text{C}$  and the V-doped  $\text{NiFe}_2\text{O}_4$  reactant powders were sintered at  $1100^\circ\text{C}$  after being calcined at  $600^\circ\text{C}$ .

According to the optimum parameters determined in terms of properties, the V-doped  $\text{NiFe}_2\text{O}_4$  ferrites were produced as composite with a PANI base and their features were characterized. V doped  $\text{NiFe}_2\text{O}_4$ : PANI was produced by hot pressing at different ratios. Microwave absorbing composites were manufactured by using epoxy at different ratios of aniline / V-added Ni ferrite such as 1/1 and 3/1. The composites that were produced were characterized using XRD, SEM and FTIR (Bruker /Alpha -T) and VSM (Cryogenic Limited PPMS) devices. The microwave absorber performances of polyaniline- $\text{NiFe}_2\text{O}_4$ : V composites were measured with the two-port vector network analyzer (R & S FSH-K42) device in the range of 0-8 GHz.

## Experimental

### *Preparation of V doped Nickel ferrite*

V doped  $\text{NiFe}_2\text{O}_4$  powder was produced using mixed oxide technique. NiO (AcrosOrganic: 99.9%),  $\text{Fe}_2\text{O}_3$  (Sigma-Aldrich: 99%) and  $\text{V}_2\text{O}_5$  (Sigma-Aldrich: 99.9%) powders were mixed in stoichiometric amounts, according to the  $\text{NiFe}_{2-x}\text{V}_x\text{O}_4$  compositions, in an ethanol medium inside a plastic container for 20h where x was selected as 0.1, 0.2, 0.3. After the slurries were dried at  $100^\circ\text{C}$  for 24h, they were calcined at  $600^\circ\text{C}$  for 4h in a tightly closed alumina crucible to prevent evaporation losses, which were checked by weighing the samples before and after calcination. After the calcined powders were ground in an agate mortar, they were pressed into pellets with 10 mm in diameter and 1-2 mm in thickness by using uniaxial press with 2MPa pressure. The pellets were sintered between 1000 and  $1200^\circ\text{C}$  for 4h with a heating and cooling rate of  $250^\circ\text{C}/\text{h}$  after being buried in the  $\text{NiFe}_2\text{O}_4$  powder to minimize the loss of volatile species.

The phases in the doped sintered samples were characterized by using X-ray diffractometry (D2 Phaser Bruker AXS) with Cu-  $K\alpha$  radiation ( $\lambda=1.5406\text{ \AA}$ ) in the range of  $2\theta:10-70^\circ$  and at a scan rate of  $1^\circ/\text{min}$ . The fracture surfaces of the specimens were examined in the SEM (JEOL 5910LV) at 20kV after being coated with Au/Pd alloy by sputter coater. The chemical analysis was conducted by means of dispersive spectrometry (EDS, Oxford-Inca-7274) and the SEM was used in order to identify the phases and study the microstructure.

### *Preparation of Polyaniline/ $\text{NiFe}_2\text{O}_4$ : V composites*

The Ni ferrite, which has the compositions of  $\text{NiFe}_{1.9}\text{V}_{0.1}\text{O}_{4.1}$ ,  $\text{NiFe}_{1.8}\text{V}_{0.2}\text{O}_{4.2}$ ,  $\text{NiFe}_{1.7}\text{V}_{0.3}\text{O}_{4.3}$  (account for 100 wt % and 33 wt % of aniline quantity), and the 1 ml aniline monomer was added to a 35 ml hydrochloric acid solution ( $0.1\text{ mol L}^{-1}$ ) and dispersed by mechanical stirring for 30 min. 2.49g of ammonium persulfate (APS) was dissolved in a 15 ml hydrochloric acid solution ( $1\text{ mol L}^{-1}$ ). The APS solution was then slowly added dropwise to the mixture solution mentioned above by stirring vigorously. Polymerization was carried out in an ice-water bath for 12h at  $0^\circ\text{C}$ . The composites were obtained by filtering and washing the reaction mixture with deionized water, and ethanol and being dried under vacuum at  $60^\circ\text{C}$  for 24 h. The PANI/ Ni ferrite composites with different molar ratios [Aniline/ $\text{NiFe}_{1.9}\text{V}_{0.1}\text{O}_{4.1}$ , Aniline/  $\text{NiFe}_{1.8}\text{V}_{0.2}\text{O}_{4.2}$ , and Aniline/  $\text{NiFe}_{1.7}\text{V}_{0.3}\text{O}_{4.3}$  = (3:1, 1:1)] were obtained to investigate the influence of the PANI content on the electromagnetic absorption properties.

### *Preparation of Epoxy- Polyaniline/ $\text{NiFe}_2\text{O}_4$ : V composites*

The absorbing composite materials were prepared by molding and curing the mixture of PANI/ Ni ferrite compositions powders and epoxy. The mixing ratio of specimen powders to epoxy was 2:1 by weight. Molding was carried out in a hydraulic press at 5Mpa pressure and  $100^\circ\text{C}$  for 1 h. They were pressed into pellets with 20 mm in diameter and 2 mm in thickness for reflectivity measurements.

## Results and Discussion

### *XRD Analysis of V Doped Nickel Ferrite*

The V ion was doped into  $\text{NiFe}_2\text{O}_4$  (PDF Card No: 44-1485) compound to replace Fe ion since they have close ionic radii values.

V doping into the Nickel ferrite structure was made along the  $\text{NiFe}_{2-x}\text{V}_x\text{O}_4$  composition with  $x$  value varying between  $x=0.1$  and  $0.5$ . The XRD analysis of samples sintered at  $1100^\circ\text{C}$  for 4h revealed that single phase structure was formed for the 0.1, 0.2 and 0.3 values of  $x$  (Fig. 1). The single phase formation of the powders was achieved by an appropriate calcination temperature and elimination of the possible intermediate phases by using the mixed oxide synthesis. The well homogenization of the powders enhanced the diffusion process during the heat treatment. XRD results indicate that there is no secondary phase in the powders except 0.5 mol% V doped sample. The second phase, that is  $\text{V}_2\text{O}_5$  (PDF Card No: 053-0538), started to appear together with 0.5 mol % V doping sample. These results show that V solubility had at limit between  $x=0.3$  and  $x=0.5$  in Nickel ferrite.

V element's ionic radii is greater than Fe element's, therefore when V element is doped into  $\text{NiFe}_2\text{O}_4$  compound to replace Fe ion, peak positions change. As the doping content increases within the solubility limit, peak positions change linearly to the right, however the main profile, the peak positions of  $\text{NiFe}_2\text{O}_4$  stays the same.

Furthermore,  $\text{NiFe}_2\text{O}_4$  formation strongly depends on temperature and high temperatures are required to form single phase  $\text{NiFe}_2\text{O}_4$ . The formation temperatures of single phase  $\text{NiFe}_2\text{O}_4$  were also strongly dependent on the type of doping.

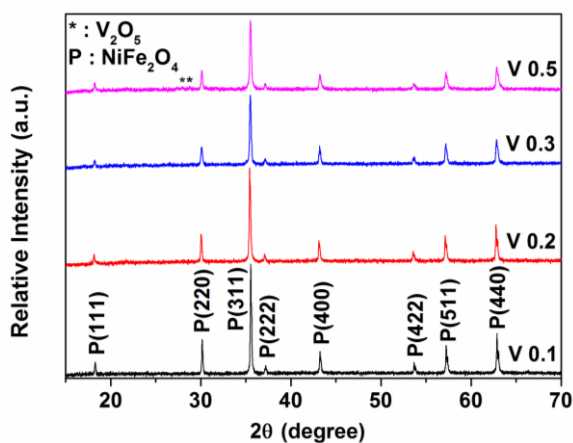
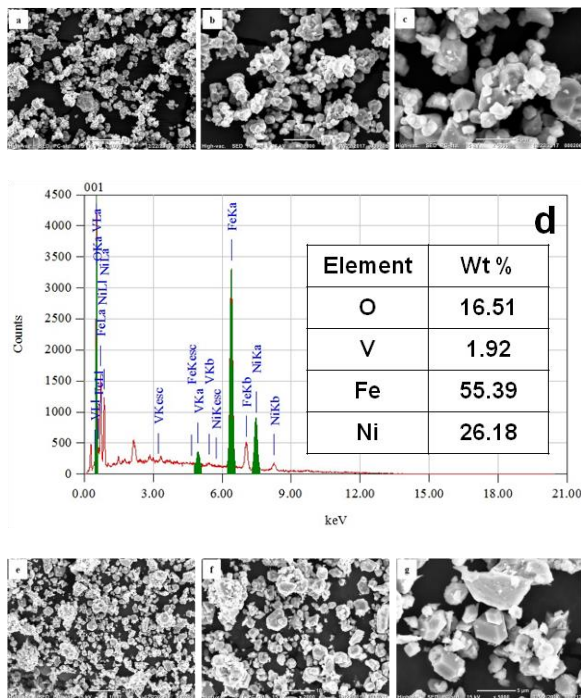


Fig. 1: XRD patterns of V doped  $\text{NiFe}_{2-x}\text{V}_x\text{O}_4$  composition with  $x=0.1, 0.2, 0.3, 0.5$  sintered during 4h at  $1100^\circ\text{C}$ .

#### SEM Analysis of V Doped Nickel Ferrite

SEM images for the V doped Nickel ferrite structure showed that there is only a single phase (Fig. 2 a, b, c) for  $x=0.1$ . However, when the  $x$  value was increased to 0.5, a large amount of secondary phase was detected in the structure (Fig.2 e, f, g). While one of the phases was determined as V containing Nickel ferrite, the other one was  $\text{V}_2\text{O}_5$ . The EDS analysis was performed and the images were shown in Fig.2 (d, h). EDS analysis applied to V ( $x=0.1$ ) doped  $\text{NiFe}_2\text{O}_4$  particles gave similar results to the theoretical composition of V doped  $\text{NiFe}_2\text{O}_4$  (%26.18 Ni, %55.39 Fe, %16.51 O, %1.92 V). The content of secondary phase increased along with the increasing in V content (Fig. 2h). SEM investigations of the samples revealed that increasing dopant concentration of V increased the grain size little. By the EDS analysis applied to the secondary phase, it is understood that the ratio of V in the structure has increased.

By examining from the grain size perspective with SEM, average grain size is between 1.5 and  $4\ \mu\text{m}$  (V doped Ni ferrite,  $x=0.1$ ). When V content increases grain size is between  $1.8\ \mu\text{m}$  and  $5\ \mu\text{m}$  (V doped Ni ferrite,  $x=0.5$ ). In addition, the secondary phase formation, observed from EDS chemical analysis was also in good concordance with the XRD results.



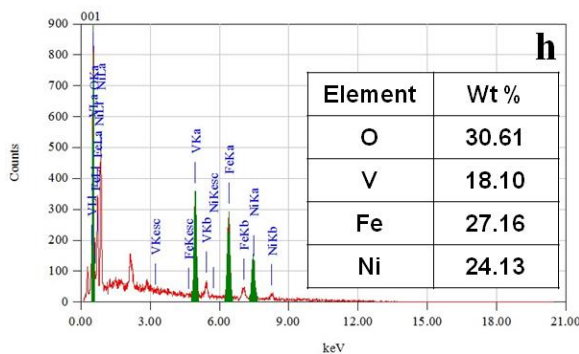


Fig. 2: SEM images of V doped  $\text{NiFe}_{2-x}\text{V}_x\text{O}_4$  sintered at  $1100^\circ\text{C}$  for 4h a)  $x=0.1$  at  $\times 1.000$ , b)  $x=0.1$  at  $\times 2.000$ , c)  $x=0.1$  at  $\times 5.000$  for d) EDS analysis of V doped  $\text{NiFe}_{2-x}\text{V}_x\text{O}_4$ ,  $x=0.1$  at  $\times 1.000$  e)  $x=0.5$  at  $\times 1.000$  f)  $x=0.5$  at  $\times 2.000$  g)  $x=0.5$  at  $\times 5.000$  h) EDS analysis of V doped  $\text{NiFe}_{2-x}\text{V}_x\text{O}_4$   $x=0.5$  at  $\times 5.000$ , the secondary phase ( $\text{V}_2\text{O}_5$ ) for  $x=0.5$ .

#### Fourier-transform IR (FTIR) spectroscopy analysis of V Doped Nickel Ferrite

The formation of the structure of nickel ferrite doped with V samples was also proved by FTIR (Fourier-transform infrared spectroscopy) spectra in the range of  $4000\text{--}500\text{ cm}^{-1}$ . Figure 3 shows the (FTIR) results of V doped  $\text{NiFe}_2\text{O}_4$  and Aniline/ (V doped  $\text{NiFe}_{2-x}\text{V}_x\text{O}_4$  for  $x=0.1, 0.3$ ) = 1/1, 1/3), composites. The different characteristic peaks of the synthesized materials were investigated by FTIR and some information was obtained about the chemical bonding in the structure. The FTIR spectra of the  $\text{NiFe}_2\text{O}_4$ , PANI and  $\text{V}_x$ ,  $\text{NiFe}_{2-x}\text{V}_x\text{O}_4$  composites that prepared with different amounts of V were recorded to determine the chemical structure of the samples. Figure 3 also shows the comparison between the observed absorption bands of free V and the observed absorption bands of PANI/ $\text{NiFe}_2\text{O}_4$  /V nanocomposites., The metal ions in ferrites are generally located in two different sub-lattice, designated as tetrahedral and octahedral sites according to the geometrical configuration of the nearest neighbors of oxygen [42]. As shown in Figure 3, the spectra, revealing the characteristic absorption peaks of the  $\text{NiFe}_2\text{O}_4$  was observed below  $600\text{ cm}^{-1}$  for all the samples and they can be attributed to the Ni-O bond or Fe - O stretching vibrations. Polymerization of the aniline can be confirmed by the presence of spectral peaks near  $1473$  and  $1552\text{ cm}^{-1}$  for PANI doped samples, which are attributed to the stretching C=C and C=N modes for quinonoid and benzenoid units of PANI, respectively, for the HCl

doped PANI [43]. The  $1236\text{ cm}^{-1}$  and  $1239\text{ cm}^{-1}$  are assigned to C-N stretching of the benzenoid ring. The band at  $1289\text{ cm}^{-1}$  that are characteristic peaks of PANI are attributed to C-N stretching mode for the benzenoid units in terms of the all samples containing PANI. These stretching vibrations can correspond to the stretching vibrations of metal-oxygen at the tetrahedral and octahedral site, respectively [40, 44]. However, the FTIR spectra of the composite samples showed that the peaks of PANI doped samples shifted to higher wave number ( $479\text{ cm}^{-1}$  and  $563\text{ cm}^{-1}$ ). These results indicated that there were some interactions between PANI chains and nickel ferrite particles [45]. Also, the hydrogen bonding interaction between the polyaniline chains and the oxygen atoms on the ferrite surface occurs in the composites, which make ferrite particles be embedded into polymer chain of PANI [46]. The peak at  $1289\text{ cm}^{-1}$  belongs to the C-N stretching of secondary amine in polymer main chain [43] and the  $1239\text{ cm}^{-1}$  for V 0.1 PANI 1/1 is the C- N stretching of benzenoid ring [47]. These specific peaks in the functional group region of the FTIR are observed at slightly higher frequency than their actual values because of the interaction with nickel ferrite moiety [43]. The peak  $1631\text{ cm}^{-1}$  for V 0.1 and V 0.3 refers to O-H stretching vibration or bending mode of  $\text{H}_2\text{O}$  molecules. The band at  $1126\text{ cm}^{-1}$  for V 0.1 can be assigned to bending vibration of C-H mode. [43, 44].  $574\text{ cm}^{-1}$  can be attributed to Ni-O bond for V 0.3 PANI 1/1 [40]. The band at  $1014\text{ cm}^{-1}$  was associated with the V=O stretching vibration [48]. The band at  $524\text{ cm}^{-1}$  represents the V-O-V stretching vibration [49]. The band at  $840\text{ cm}^{-1}$  was attributed to the coupled vibration between V=O and V -O- V. The band at  $1100\text{ cm}^{-1}$  represents the V=O .The bands around  $995\text{--}1050\text{ cm}^{-1}$  can be attributed to the stretching of short V=O bonds. [50]. The strong peaks in the region at  $563\text{ cm}^{-1}$  and  $479\text{ cm}^{-1}$  are related to the symmetric V-O-V stretching mode [51]. The band at  $1022\text{ cm}^{-1}$  was assigned to the V=O stretching vibration, the IR band of V=O in crystalline  $\text{V}_2\text{O}_5$  was showed at  $1020\text{--}1025\text{ cm}^{-1}$  [52].  $1558\text{ cm}^{-1}$  is the C=N quinonoid stretching mode of vibration [47].

Using of the V causes to the shift of some bands in the PANI- $\text{NiFe}_2\text{O}_4$  nanocomposites. These differences indicate strong interactions between PANI,  $\text{NiFe}_2\text{O}_4$ , and ionic liquid in the composites. The interaction between PANI and  $\text{NiFe}_2\text{O}_4$  is thought to be an N-O hydroxyl bond interaction, so the separation of PANI and  $\text{NiFe}_2\text{O}_4$  from each other is difficult. In addition, it can be seen that the peaks in samples that does not contain the PANI are broader than the samples with V-PANI.

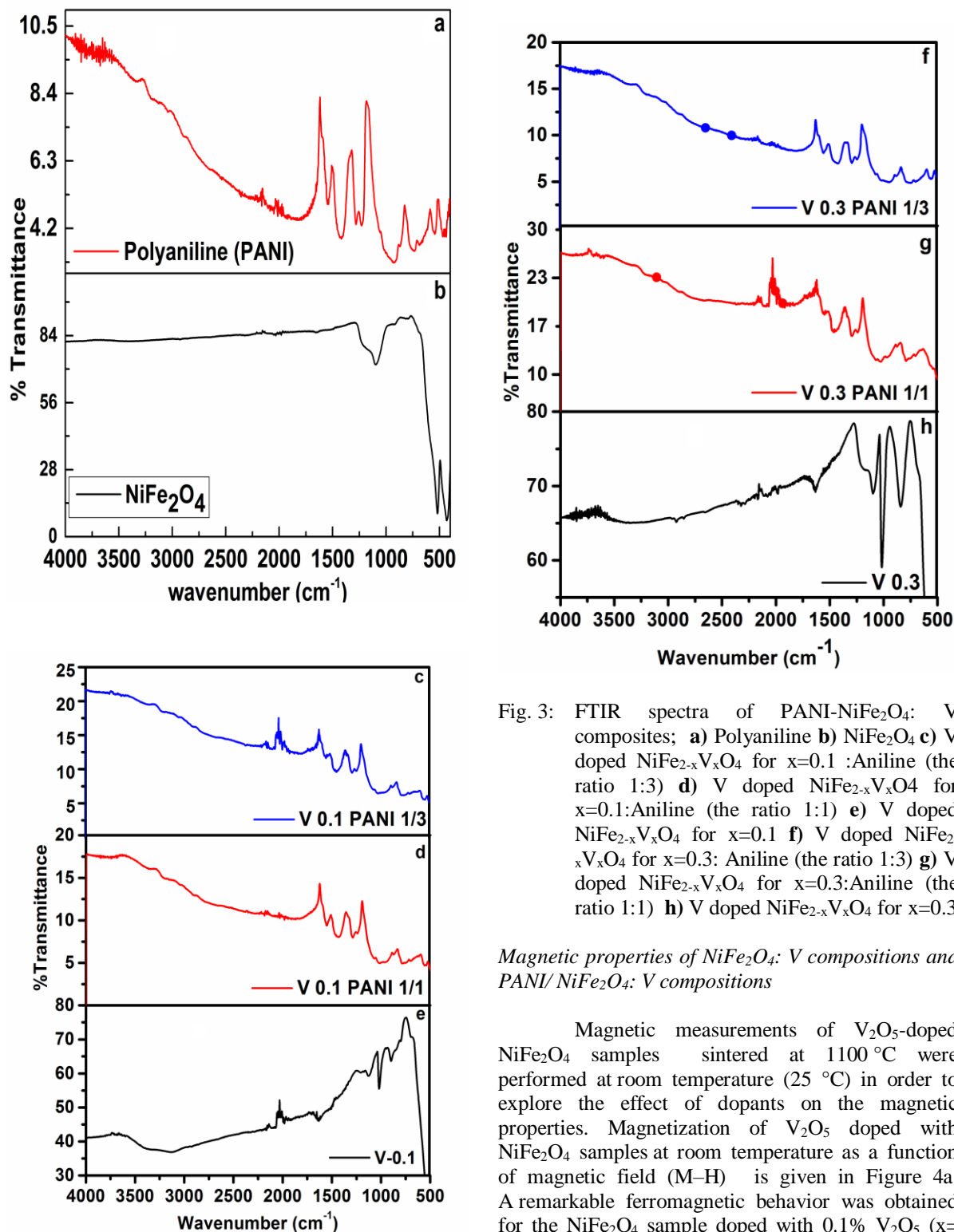


Fig. 3: FTIR spectra of PANI-NiFe<sub>2</sub>O<sub>4</sub>: V composites; **a**) Polyaniline **b**) NiFe<sub>2</sub>O<sub>4</sub> **c**) V doped NiFe<sub>2-x</sub>V<sub>x</sub>O<sub>4</sub> for x=0.1 :Aniline (the ratio 1:3) **d**) V doped NiFe<sub>2-x</sub>V<sub>x</sub>O<sub>4</sub> for x=0.1:Aniline (the ratio 1:1) **e**) V doped NiFe<sub>2-x</sub>V<sub>x</sub>O<sub>4</sub> for x=0.1 **f**) V doped NiFe<sub>2-x</sub>V<sub>x</sub>O<sub>4</sub> for x=0.3: Aniline (the ratio 1:3) **g**) V doped NiFe<sub>2-x</sub>V<sub>x</sub>O<sub>4</sub> for x=0.3:Aniline (the ratio 1:1) **h**) V doped NiFe<sub>2-x</sub>V<sub>x</sub>O<sub>4</sub> for x=0.3

*Magnetic properties of NiFe<sub>2</sub>O<sub>4</sub>: V compositions and PANI/NiFe<sub>2</sub>O<sub>4</sub>: V compositions*

Magnetic measurements of V<sub>2</sub>O<sub>5</sub>-doped NiFe<sub>2</sub>O<sub>4</sub> samples sintered at 1100 °C were performed at room temperature (25 °C) in order to explore the effect of dopants on the magnetic properties. Magnetization of V<sub>2</sub>O<sub>5</sub> doped with NiFe<sub>2</sub>O<sub>4</sub> samples at room temperature as a function of magnetic field (M-H) is given in Figure 4a. A remarkable ferromagnetic behavior was obtained for the NiFe<sub>2</sub>O<sub>4</sub> sample doped with 0.1% V<sub>2</sub>O<sub>5</sub> (x=0.1) which has saturation magnetization (M<sub>s</sub>) of about 41.1 emu/g. As the concentration of the dopant element increased to x=0.2, the saturation magnetization decreased to almost 38.7 emu/g. As the concentration of the dopant

element increased to  $x=0.3$ , it was observed a further decrease in  $M_s$  at almost 27.4 emu/g. In general, as the dopant element increased, the saturation magnetization decreased.

The magnetization of spinel ferrite can be explained by the Neel's molecular field model. According to this model, the exchange interaction between A-B sites is stronger than A-A and B-B interactions. For  $x=0.1$ , the concentration of  $Fe^{+3}$  ions at octahedral B-sites decreases due to the accumulation of  $V_2O_5$  ions on B-sites. Hence, the change in the magnetic structure results in a decrease in saturation magnetization. The decrease in the magnetization at  $x \geq 0.2$  may be attributed to the distribution of nonmagnetic  $V_2O_5$  ions in A and B sites.

When the  $NiFe_2O_4$  sample was doped with  $x=0.5 V_2O_5$ , a slight increase up to 28.4 emu/g was noted in  $M_s$ . As the PANI concentration decreased from 1:1 to 1:3, saturation magnetization also decreased as expected. The magnetic field dependent magnetization at 1100 °C for  $V_2O_5$  doped  $NiFe_2O_4$  samples ( $x=0.1$ ) with different PANI concentrations (1/3 and 1/1) is shown in Figure 4 b. Both samples showed different ferromagnetic behavior. While the  $M_s$  for the sample with polyaniline concentration 1/3 appeared less with about the value of 10.7 emu/g, the sample with polyaniline concentration 1/1 showed higher  $M_s$  with about value of 18.9 emu/g. Similarly,  $V_2O_5$  doped  $NiFe_2O_4$  samples ( $x=0.3$ ) with different polyaniline concentration (1/3 and 1/1) showed ferromagnetic behavior with  $M_s = 6.6$  and 18.8 emu/g respectively.

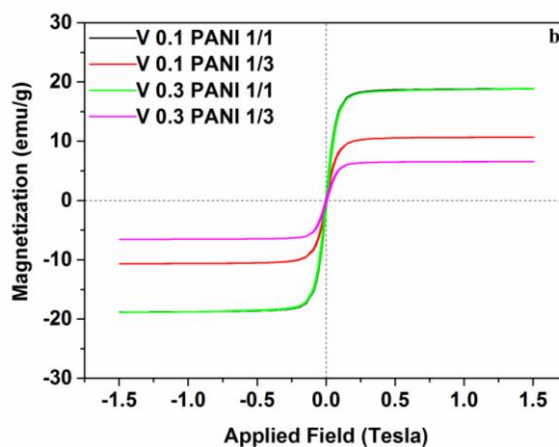
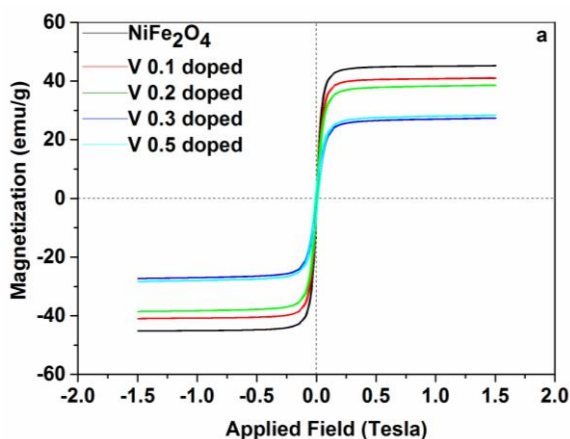


Fig. 4: a ) Magnetization curves for V doped  $NiFe_2O_4$  ( $x=0.1, 0.2, 0.3, 0.5$ ) heat treated at 1100 °C for 4 h.  
b ) Magnetization curves for V doped  $NiFe_2O_4$  ( $x=0.1, 0.3$ ) using polyaniline (1/3, 1/1) heat treated at 1100 °C for 4 h.

#### Reflectivity Measurements of V Doped Nickel Ferrite

Figure 5 shows the frequency dependence of the reflection loss of the Epoxy- PANI/ $NiFe_2O_4$ : V composites in the frequency range of 0-8 GHz. Among the PANI- $NiFe_2O_4$ : V composites, It can be seen that epoxy- $NiFe_2O_4$ : V composites /Aniline: 1/1 has more observable effect on microwave absorption properties than epoxy-  $NiFe_2O_4$ : V composites/Aniline: 1/3. The PANI/ $Ni$  ferrite compositions ( $NiFe_{1.9}V_{0.1}O_{4.1}$ /Aniline: 1/1) powders and epoxy showed only two bands with -36.32 dB and -26.14 dB at 5.68 GHz and at 1.82 GHz respectively. The epoxy-PANI/  $Ni$  ferrite compositions ( $NiFe_{1.9}V_{0.1}O_{4.1}$ / Aniline:1/3) reach to -23.48 dB at 7.31 GHz in reflection loss (Fig5.a). The compositions reach to a reflectivity of -28.39 dB at 6.22 GHz for epoxy-PANI/ $Ni$  ferrite compositions ( $NiFe_{1.7}V_{0.3}O_{4.3}$  / Aniline: 1/1) (Fig5.b). When nickel ferrite powder content decreases, PANI/  $Ni$  ferrite compositions ( $NiFe_{1.7}V_{0.3}O_{4.3}$  / Aniline: 1/3) reach to the -42.17 dB and -35.61 dB at 7.02 GHz and at 5.63 GHz, respectively. In addition, this composite material achieves a reflection less than -10 dB in the frequency band between 3.94 GHz and 8 GHz. The best overall reflection loss performance was achieved with the  $NiFe_{1.9}V_{0.1}O_{4.1}$ /Aniline: 1/1 composition (Fig5.a) which shows a value less than -20 dB in the frequency band between 5.28 GHz and 8 GHz. Moreover, it achieves a reflection less than -10 dB in the frequency band between 3.63 GHz and 8 GHz.

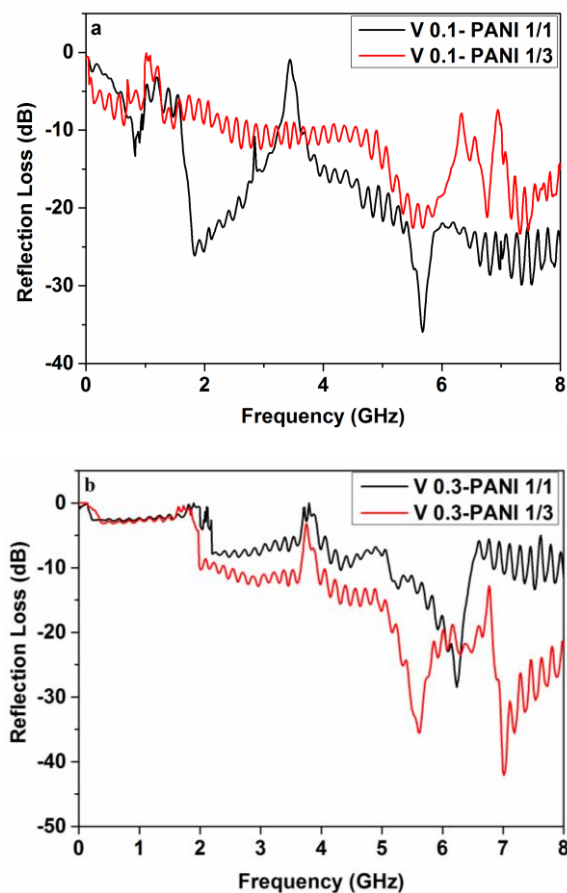


Fig. 5: Microwave absorption properties of the Epoxy- PANI-NiFe<sub>2</sub>O<sub>4</sub>: V composites **a)**  $x=0.1$ , V- added Ni ferrite /Aniline compositions of NiFe<sub>1.9</sub>V<sub>0.1</sub>O<sub>4.1</sub> weight ratio was changed as 1:1, 1:3 **b)**  $x=0.3$ , V-added Ni ferrite /Aniline compositions of NiFe<sub>1.7</sub>V<sub>0.3</sub>O<sub>4.3</sub> weight ratio was changed as 1:1, 1:3.

In addition, PANI improves the matching impedance on the transmissions between the ingredients of the composites.

It is seen that the EM absorber property is mainly due to the magnetic spinel ferrite Ni. Meanwhile, the sharp absorption peaks appear due to the effect of conductive polymer PANI. Conducting polymer matrix (PANI) has been used in particular to reduce the effect of existing eddy currents, since the permeability of magnetic materials at high frequencies will reduce Eddy currents generated by EM waves. PANI creates electrical loss. It was mixed with spinel magnetic materials such as Ni and with the magnetic absorption feature provide to control EM absorptivity. In fact, the changes such as the saturation magnetization, magnetocrystalline

anisotropy, dielectric properties and resonance frequency shifting of the material were provided. So, the effect of this is apparent in the material, and the absorption peak is shifted to the high frequency region, Reflection loss curves can possess little blips.

In Fig. 5a part, the effect of PANI is less than the magnetic powder effect. In 5b part, when powder amount  $V(x=0.3)$ , the solubility increased when V element settles into NiFe<sub>2</sub>O<sub>4</sub>, structured its environment according to itself, increased the wave interference by the increasing surface area and increased the absorption. Matching of Impedance has been achieved by using PANI. PANI effect has increased the absorption.

New V doped NiFe<sub>2</sub>O<sub>4</sub> and new V doped NiFe<sub>2</sub>O<sub>4</sub>: PANI were produced, V doped NiFe<sub>2</sub>O<sub>4</sub>: PANI based composite have a high absorption ratio for electromagnetic waves in a broadwidth range, Magnetic and absorbing properties of the new composites are adjusted by controlling the V doped ferrite and PANI content in this method. Studies show that doping and PANI affect in electrical and magnetic structure. V affected permeability of material and contributes to the reflection.

## Conclusion

V doped NiFe<sub>2</sub>O<sub>4</sub> was produced along with NiFe<sub>2-x</sub>V<sub>x</sub>O<sub>4</sub> compositions by using mixed oxide technique and PANI-NiFe<sub>2</sub>O<sub>4</sub>:V composites were produced for the first time in literature, to our knowledge. The V solubility in NiFe<sub>2</sub>O<sub>4</sub> was much higher ( $x=0.3$ ). The secondary phase could be identified as V<sub>2</sub>O<sub>5</sub> in V doping.

SEM investigation also confirmed the XRD results, as it gave only single phase below  $x=0.3$  for V doping. The minimum reflection point shifts toward higher frequency with a decrease of PANI content for epoxy -PANI/ NiFe<sub>2</sub>O<sub>4</sub>: V compositions. Among epoxy-PANI/NiFe<sub>2</sub>O<sub>4</sub>:V compositions, the NiFe<sub>1.9</sub>V<sub>0.1</sub>O<sub>4.1</sub>/Aniline:1/1 and the NiFe<sub>1.7</sub>V<sub>0.3</sub>O<sub>4.3</sub>/Aniline:1/3 gave the best overall reflection performance in the frequency band between 3.94 GHz and 8.GHz.

The magnetic value in the lowest V doped NiFe<sub>2</sub>O<sub>4</sub> structure gave better results, and the amount of polyaniline played an important role in determining the absorber values.

The microwave absorption property was obtained as 7.02 GHz and 2.0 mm in thickness with the minimum RL of -42.17 dB by

NiFe<sub>1.7</sub>V<sub>0.3</sub>O<sub>4.3</sub>/Aniline:1/3 composite. Microwave absorbing properties can be modulated simply by controlling the content of PANI and the effect of V dopant on the samples for the required frequency bands. Due to the easy and low cost preparation methods and better reflectivity performance, the PANI / V doped Nickel ferrite composites have a promising potential as microwave absorber. The dopants and Polyaniline were used to improve the microwave absorber properties of NiFe<sub>2</sub>O<sub>4</sub>.

Microwave absorbing properties of V doped NiFe<sub>2</sub>O<sub>4</sub>: PANI compositions show a consistent variation with high V doping amounts. The best reflection loss performance is obtained from NiFe<sub>1.9</sub>V<sub>0.1</sub>O<sub>4.1</sub>/Aniline: 1/1 composition at the value of less than -20 dB and between 5.28 GHz and 8GHz. The content of polyaniline plays an important role in variation the absorbing properties. The microwave absorbing properties of the V doped NiFe<sub>2</sub>O<sub>4</sub>: PANI compositions can be investigated for a broader concentration range of V dopant below 0.5 than those in this study.

V doped NiFe<sub>2</sub>O<sub>4</sub>: PANI can be considered as a candidate for microwave absorbers Dopants and polyaniline content have been used to improve the microwave absorbing properties of NiFe<sub>2</sub>O<sub>4</sub>. Dopant formation is another area of interest concerned with Nickel ferrite. The absorber properties of Nickel ferrite can be improved by using various dopant elements, and polymers. The microwave absorption properties of PANI -single phase doped NiFe<sub>2</sub>O<sub>4</sub> at high frequencies may also be determined.

#### Acknowledgment

This study was supported by the Scientific Research Projects Office (BAP) of Istanbul Technical University (Project Number: 39309). This study is attributed to Prof. Dr. Ayhan Mergen who passed away in August, 2017. The authors would like to express their gratitude to him for his friendship, comments and faithful collaboration.

#### References

- S. Kamba, D Noujni, A. Pashkin, J. Petzelt, R.C. Pullar, A. K. Axelsson and N. McN Alford, Low temperature microwave and THz dielectric response in novel microwave ceramics, *J. Eur. Ceram. Soc.*, **26**, 1845 (2006).
- G. Mu, H. Shen, J. Qiu and M Gu, Microwave absorption properties of composite powders with low density, *Appl. Surf. Sci.*, **253**, 2278 (2006).
- Y. P. Wu, C. K. Ong, G. Q. Lin and Z. W. Li, Improved microwave magnetic and attenuation properties due to the dopant V<sub>2</sub>O<sub>5</sub> in W-type barium ferrites, *J. Phys. D: Appl. Phys.*, **39**, 2915 (2006).
- S. Geetha, K. K. S. Kumar ve D.C. Trivedi, Polyaniline reinforced conducting E-glass fabric using 4-chloro-3-methyl phenol as secondary dopant for the control of electromagnetic radiations, *Compos. Sci. Technol.*, **65**, 973 (2005).
- D. S. Li, T. Horikawa, J. R. Liu, M. Itoh and K. Machida, Electromagnetic wave absorption properties of iron/rare earth oxide composites dispersed by amorphous carbon powder, *J. Alloys and Compd.*, **408**, 1429 (2006).
- S. P. Pawar, M. Gandi and S. Bose, High performance electromagnetic wave absorbers derived from PC/SAN blends containing multiwall carbon nanotubes and Fe<sub>3</sub>O<sub>4</sub> decorated onto graphene oxide sheets, *RSC Adv.*, **44**, 37319 (2016).
- A. Hajalilou, M. Hashim, R. Ebrahimi-Kahrizsangi, H. Mohamed Kamari, N. Sarami, Synthesis and structural characterization of nano-sized nickel ferrite obtained by mechanochemical process, *Ceram. Int.*, **40**, 5881 (2014).
- C. Xiangfeng, J. Dongli and Z. Chenmou, The preparation and gas-sensing properties of NiFe<sub>2</sub>O<sub>4</sub> nanocubes and nanorods, *Sens. Actuators B*, **123**, 793 (2007).
- E. Hasmonay, J. Depeyrot, M. H. Sousa, F. A. Tourinho, J. C. Bacri, R. Perzynski, Y. L. Raikher and I. Rosenman, Magnetic and optical properties of ionic ferrofluids based on nickel ferrite nanoparticles, *J. Appl. Phys.*, **88**, 6628 (2000).
- S. Rana, R. S. Srivastava, M. M. Sorensson and R. D. K. Misra, Synthesis and characterization of nanoparticles with magnetic core and photocatalytic shell: Anatase TiO<sub>2</sub>-NiFe<sub>2</sub>O<sub>4</sub> system, *Mater. Sci. Eng. B*, **119**, 144 (2005).
- Y. L. Raikher, V. I. Stepanov, J. Depeyrot, M. H. Sousa, F. A. Tourinho, E. Hasmonay and R. Perzynski, Dynamic optical probing of the magnetic anisotropy of nickel-ferrite nanoparticles, *J. Appl. Phys.* **96**, 5226 (2004).
- D. H. Han, H. L. Luo and Z. Yang, Remanent and anisotropic switching field distribution of plate like Ba-ferrite and acicular particulate recording media, *J. Magn. Magn. Mater.*, **161**, 376 (1996).
- A. K. Giri, K. Pellerin, W. Pongsaksawad, M. Sorescu and S. A. Majetich, Effect of Light on the Magnetic Properties of Cobalt Ferrite

- Nanoparticles, *IEEE Trans. Magn.*, **36**, 3029 (2000).
14. C. H. Cunningham, T. Arai, P. C. Yang, M. V. McConnell, J. M. Pauly and S. M. Connolly, Positive contrast magnetic resonance imaging of cells labeled with magnetic nanoparticles, *Magn. Reson. Med.*, **53**, 999 (2005).
  15. T. J. Yoon, J. S. Kim, B. G. Kim, K. N. Yu, M. H. Cho and J. K. Lee, Multifunctional nanoparticles possessing a “magnetic motor effect” for drug or gene delivery, *Angew. Chem.* **117**, 1092 (2007).
  16. P. Sivakumar, R. Ramesh, A. Ramanand, S. Ponnusamy and C. Muthamizhchelvan. Synthesis and characterization of NiFe<sub>2</sub>O<sub>4</sub> nanoparticles and nanorods, *J. Alloys and Compd.*, **563**, 6 (2013).
  17. Y. Kinemuchi, K. Ishizaka, H. Suematsu, W. Jiang, K. Yatsui, Magnetic properties of nanosize NiFe<sub>2</sub>O<sub>4</sub> particles synthesized by pulsed wire discharge, *Thin-Solid-Films*, **407**, 109 (2002).
  18. D. R. Patil and B. K. Chougule, Effect of copper substitution on electrical and magnetic properties of NiFe<sub>2</sub>O<sub>4</sub> ferrite, *Mater. Chem. Phys.*, **117**, 35 (2009).
  19. X. G. Liu, J. J. Jiang, D. Y. Geng, B. Q. Li, W. Liu and Z. D. Zhang, Dual nonlinear dielectric resonance and strong natural resonance in Ni/ZnO nanocapsules, *Appl. Phys. Lett.*, **94**, 053119 (2009).
  20. T. Wei, C. Q. Jin, W. Zhong and J. M. Liu, High permittivity polymer embedded with Co/ZnO core/shell nanoparticles modified by organophosphorus acid, *Appl. Phys. Lett.*, **94**, 22907 (2007).
  21. X. G. Liu, D. Y. Geng, H. Meng, P. J. Shang and Z. D. Zhang, Microwave-absorption properties of ZnO-coated iron nanocapsules, *Appl. Phys. Lett.*, **92** (2008).
  22. X. Lu, G. Liang, Y. Zhang and W. Zhang, Synthesis of FeNi<sub>3</sub>/(Ni<sub>0.5</sub>Zn<sub>0.5</sub>)Fe<sub>2</sub>O<sub>4</sub> nanocomposite and its high frequency complex permeability, *Nanotechnology.*, **18**, 015701 (2006).
  23. L. G. Yan, J. B. Wang, X. H. Han, Y. Ren, Q. F. Liu and F. S. Li, Enhanced microwave absorption of Fe nanoflakes after coating with SiO<sub>2</sub> nanoshell, *Nanotechnology.*, **21**, 095708 (2010).
  24. S. H. Hosseini, S. H. Mohseni, A. Asadnia and H. Kerdari, Synthesis and Microwave Absorbing Properties of Polyaniline/MnFe<sub>2</sub>O<sub>4</sub> Nanocomposite, *J. Alloys and Compd.*, **509**, 4682 (2011).
  25. H. Jianjun, D. Yuping, Z. Jia, J. Hui, L. Shunhua, L. Weiping, MnO<sub>2</sub>/Polyaniline Composites: Preparation, Characterization, and Applications in Microwave Absorption, *Physica B*, **406**, 1950 (2011).
  26. M. Pardavi-Horvath, Microwave applications of soft ferrites, *J. Magn. Magn. Mater.* **215**, 171 (2000).
  27. A. Verma, A. K. Saxena and D. C. Dube, Microwave permittivity and permeability of ferrite-polymer thick films, *J. Magn. Magn. Mater.* **263**, 228 (2003).
  28. S. B. Cho, D. H. Kang and J. H. Oh, Relationship between magnetic properties and microwave-absorbing characteristics of NiZnCo ferrite composites, *J. Mater. Sci.*, **31**, 4719 (1996).
  29. G. K. S. Prakash, P. Suresh, F. Viva and G. A. Olah, Novel single step electrochemical route to  $\gamma$ -MnO<sub>2</sub> nanoparticle-coated polyaniline nanofibers: thermal stability and formic acid oxidation on the resulting nanocomposites. *J. Power Sources.*, **181**, 79 (2008).
  30. P. Zhang, X. J. Han, L. L. Kang, R. Qiang, W. W. Liu and Y. C. Du, Synthesis and characterization of polyaniline nanoparticles with enhanced microwave absorption, *RSC Adv.*, **3**, 12694 (2013).
  31. K. T. Mathew, A. V. Praveen Kumar and H. John, Polyaniline and Polypyrrole with PVC content for effective EMI shielding, *IEEE Int. Symp. Electromag. Compatibility*, 443 (2006).
  32. D. Yuping, L. Shunhua, G. Hongtao, Investigation of electrical conductivity and electromagnetic shielding effectiveness of polyaniline composite, *STAM journal.*, **6**, 513 (2005).
  33. S. Thirumalairajan, K. Girija, V. Ganesh, D. Mangalaraj, C. Viswanathan, N. Ponpandian, Novel synthesis of LaFeO<sub>3</sub> nanostructure dendrites: a systematic investigation of growth mechanism, properties, and biosensing for highly selective determination of neurotransmitter compounds. *Cryst. Growth Des.*, **13**, 291 (2013).
  34. F. Meng, X. Wang, D. Jiang and R. Ma, Microwave Absorbing and Magnetic Properties of the polyaniline Co<sub>0.7</sub>Cr<sub>0.1</sub>Zn<sub>0.2</sub>Fe<sub>2</sub>O<sub>4</sub> Composites, *Mater-Sci-Medzg.*, **22**, 354 (2016).
  35. C. C. Yang, Y. J. Gung, W. C. Hung, T. H. Ting, K. H. Wu, Infrared and Microwave Absorbing Properties of BaTiO<sub>3</sub>/Polyaniline and BaFe<sub>12</sub>O<sub>19</sub>/Polyaniline *Compos. Sci. Technol.*, **70**, 466 (2010).
  36. S. U. Rehman, J. Liu, R. Ahmed and H. Bi, Synthesis of composite of ZnO spheres with

- polyaniline and their microwave absorption properties, *J. Saudi Chem. Soc.*, **4**, 1 (2018).
37. K. Singh, A. Ohlan, V. H. Pham, S. Varshney, J. Jang, S. H. Hur, W. M. Choi, M. Kumar, S. K. Dhawan, B. S. Kong, J. S. Chung, Nanostructured graphene/Fe<sub>3</sub>O<sub>4</sub> incorporated polyaniline as a high performance shield against electromagnetic pollution, *Nanoscale*, **5**, 2411 (2013).
  38. X. J. Wang, F. Wang, C. Gao and D. Sun, Preparation and electromagnetic wave absorption properties of carbon nanotubes-titanium dioxide nanoparticles, *Adv.Mater. Res.* **457**, 225 (2012).
  39. G. Z. Wang, Z. Gao, G. P. Wan, S. W. Lin, P. Yang and Y. Qin, High densities of magnetic nanoparticles supported on graphene fabricated by atomic layer deposition and their use as efficient synergistic microwave absorbers, *Nano Res.* **7**, 704 (2014).
  40. A. Baykal, M. Günay, M. S. Toprak and H. Sozeri, Effect of ionic liquids on the electrical and magnetic performance of polyaniline–nickel ferrite nanocomposite, *Mater. Res. Bull.*, **48**, 378 (2013).
  41. T. H. Ting, R. P. Yu and Y. N. Jau, Synthesis and microwave absorption characteristics of polyaniline/NiZn ferrite composites in 2–40 GHz, *Mater. Chem. Phys.*, **126**, 364 (2011).
  42. A. H. Elsayed, M. S. Mohy Eldin, A. M. Elsyed, A. H. Abo Elazm, E. M. Younes and H. A. Motaweh, Synthesis and Properties of Polyaniline/ferrites Nanocomposites, *Int. J. Electrochem. Sci.*, **6**, 206 (2011).
  43. M. Khairy, Synthesis, characterization, magnetic and electrical properties of polyaniline/NiFe<sub>2</sub>O<sub>4</sub> nanocomposite, *Synthetic Met.*, **189**, 34 (2014).
  44. M. Khairy and M. E. Gouda, Electrical and optical properties of nickel ferrite/polyaniline nanocomposite, *J. Adv. Res.*, **6**, 555 (2015).
  45. A. H. Gemeay, R. G. El-Sharkawy, I. A. Mansour and A.B. Zaki, Preparation and characterization of polyaniline/manganese dioxide composites and their catalytic activity, *J. Colloid Interface Sci.*, **308**, 385 (2007).
  46. C. Leng, J. Wei, Z. Liu and J. Shi, Influence of imidazolium-based ionic liquids on the performance of polyaniline–CoFe<sub>2</sub>O<sub>4</sub> nanocomposites, *J. Alloys and Compd.*, **509**, 3052 (2011).
  47. V. B. Chanshetty, B. Sangshetty and K. Sharanappa, Surface Morphology Studies and Thermal analysis of V<sub>2</sub>O<sub>5</sub> doped polyaniline composites, *IJERA*, **2**, 611 (2012).
  48. B. R. Kamalama, B. K. Balachander and K. Sethuraman, Solvothermal Synthesis and Characterization of Reduced Graphene oxide/ Vanadium Pentoxide Hybrid nanostructures, *Mater. Today*, **3**, 2132 (2016).
  49. B. Saravanakumar, K. K. Purushothaman and G. Muralidharan, High performance supercapacitor based on carbon coated V<sub>2</sub>O<sub>5</sub> nanorods, *J. Ele. Chem.*, **758**, 111 (2015).
  50. R. L. Josephina, S. Sujaa and A. D. Raj, Comparison of optical, structural, morphological, vibrational and thermal analysis of V<sub>2</sub>O<sub>5</sub> nanobelts prepared with and without the application of constant current source from renewable energy, *Optik*, **127**, 3299 (2016).
  51. Zakharovaa, S. Galina, Y. Liub, A. N. Enyashina, X. Yang, J. Zhou, W. Jinb and W. Chen, Metal cations doped vanadium oxide nanotubes: Synthesis, electronic structure, and gas sensing properties, *Sensor Actuat. B-Chem.*, **256**, 1021 (2018).
  52. J. R. Sohn, K.C. Seo and Y. I. Pae, Characterization of Vanadium Oxide Supported on Zirconia and Modified with MoO<sub>3</sub>, *Bull. Korean Chem. Soc.*, **24**, 311 (2003).